

AN ORNITHOPTER WING DESIGN

James D. DeLaurier*

ABSTRACT

The physics of flapping-wing flight has been studied in order to gain insights on how animals fly and to assess the possibility of achieving this with a flapping-wing airplane (ornithopter). To this end, the major focus of this work has been the proof-of-concept flight tests of a remotely-piloted, engine-powered ornithopter. The level of sophistication of the analyses and laboratory experiments, which determined the design changes to the ornithopter, was driven by the results from these flight tests. Ultimately, successful sustained flight required the development of a comprehensive unsteady-aerodynamic/aeroelastic analysis complemented with wind-tunnel experiments.

RÉSUMÉ

Les caractéristiques physiques des ailes battantes ont fait l'objet de recherches visant à comprendre comment les oiseaux peuvent voler et à évaluer la possibilité de réaliser une machine à ailes battantes, ou ornithoptère. Les travaux décrits dans cette étude se sont concentrés sur les vols d'essais de validation de principe d'un ornithoptère motorisé et téléguidé. Les résultats de ces vols d'essai reposent à l'origine du niveau de complexité des analyses et des expériences en laboratoire sur lesquels sont fondées les modifications de conception de l'ornithoptère. On a finalement réussi à faire voler la machine de manière soutenue après avoir procédé à une analyse de l'aérodynamique et de l'aéroélastique interstationnaires, complétée par des expériences en soufflerie.

INTRODUCTION

The imitation of nature's flapping-wing flight has been humanity's oldest aeronautical dream. History provides numerous examples of efforts to achieve this by strapping on wings and leaping (falling) from high places. Standing well apart from these hapless efforts are the experiments of Alexander Lippisch¹ in 1929 where a human-powered ornithopter (**Figure 1**) performed extended

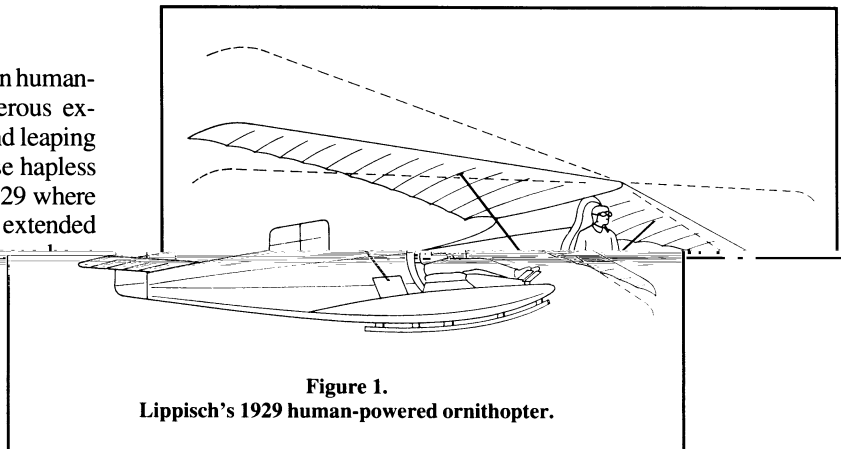


Figure 1.
Lippisch's 1929 human-powered ornithopter.

ver figures are being how for a minute. I do not think I have
n the most successful human-carrying flapping-wing flights,
er human- or engine-powered.
Much greater success has been achieved with models, starting
n Alphonse Pénaud's rubber-powered ornithopter in 1874² (**Fig-
2**). This, in fact, has been the prototype for virtually all model
ithopters built by hobbyists and manufactured as toys, with
ine-powered versions being built and successfully flown by
cival Spencer in the 1960s.³ However, even though a manufac-
er may shape and colour the model to look like a bird, as seen in
Figure 3, the aerodynamic means by which it achieves flight is very
erent from that for birds (and bats) in cruising equilibrium flight.

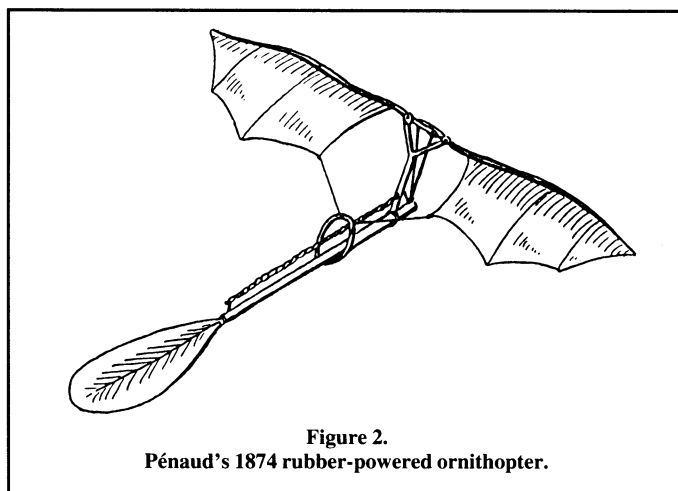


Figure 2.
Pénaud's 1874 rubber-powered ornithopter.

The Pénaud-type ornithopter is characterized by having wings
posed of a stiff leading-edge spar, to which a single sheet of
flexible material is attached (much like a traditional sail).
ribs may be added, as shown in **Figure 2**, although the
at majority of these models provide chordwise restraint only
e root, as seen in **Figure 3**. This results in a membrane wing
n considerable torsional compliance and virtually no leading-
e suction. Therefore, thrusting is generated by components
e flapping-axis direction, of the forces normal to the wing's
rds (illustrated in **Figure 4**). Experiments performed by
her, Sapuppo, and Betteridge⁴ have shown that such wings
capable of considerable thrust at low advance ratios, λ , where

$\lambda = \frac{\text{forward velocity}}{\text{maximum magnitude of tip velocity normal to flapping axis}}$

However, when the flapping axis is horizontal, these wings generate very little lift, even if cambered ribs are incorporated in the structure. Therefore, the manner in which a Pénaud-type ornithopter sustains flight is to vector the thrust, as shown in

*James D. DeLaurier is a Professor, Institute for Aerospace Studies at the University of Toronto.

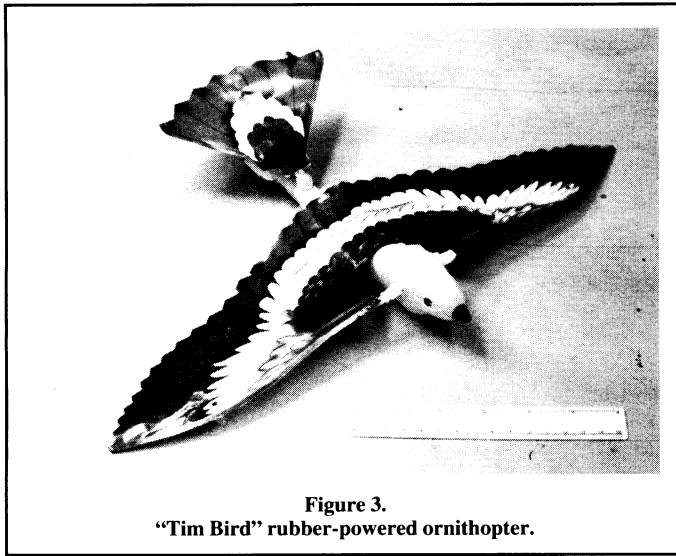


Figure 3.
"Tim Bird" rubber-powered ornithopter.

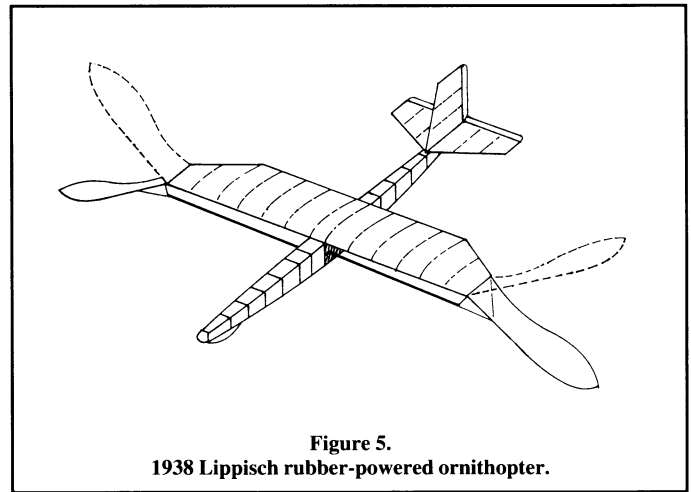


Figure 5.
1938 Lippisch rubber-powered ornithopter.

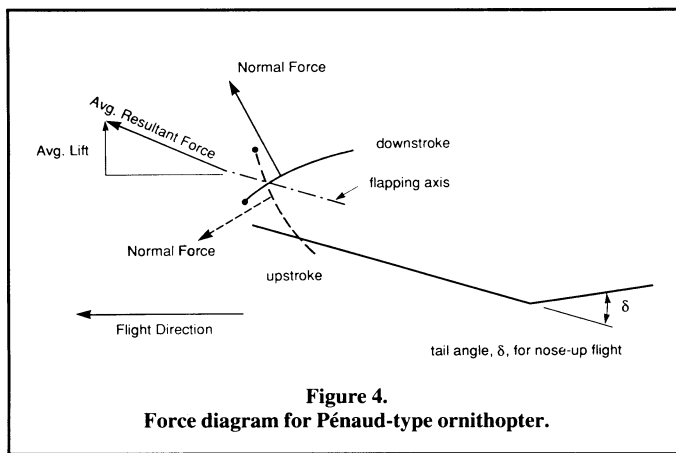


Figure 4.
Force diagram for Pénaud-type ornithopter.

Figure 4, by adjusting the mass centre and stabilizer incidence to give a large positive trim angle to the flapping axis.

The flight efficiency of such an arrangement is fairly low. This is graphically illustrated by model aviation records, which show the Pénaud-type ornithopters to have very poor flight durations compared with those for comparably-sized, propeller-driven fixed-wing models with the same amount of propulsive energy. Attempts to improve the efficiency of the Pénaud-type ornithopter have included the incorporation of fixed, cambered surfaces in the configuration, such as for the Lippisch rubber-powered model shown in Figure 5. The flapping surfaces may then be dedicated to thrust production alone, with the fixed surfaces providing the lift. A variation on this is seen in the latest competition model ornithopters (Figure 6) where the flapping surfaces are placed in the rear to provide stabilizing forces as well as thrust, and the fixed, forward wing is cambered and angled to provide efficient lift. Such configurations have increased the record duration times by an order of magnitude over the original Pénaud-type flyers; however, none of these ornithopters, including the Pénaud design, actually perform like a bird in equilibrium cruising flight.

The typical airfoils for birds and bats are thin and cambered, which means that, as for the Pénaud wing, these generate very little leading-edge suction. Hence the downstroke action (shown in Figure 7) is similar to the twisting Pénaud wing in that the normal forces produce both lift and thrust. However, unlike the Pénaud flyers, cruising birds and bats fly with their flapping axes

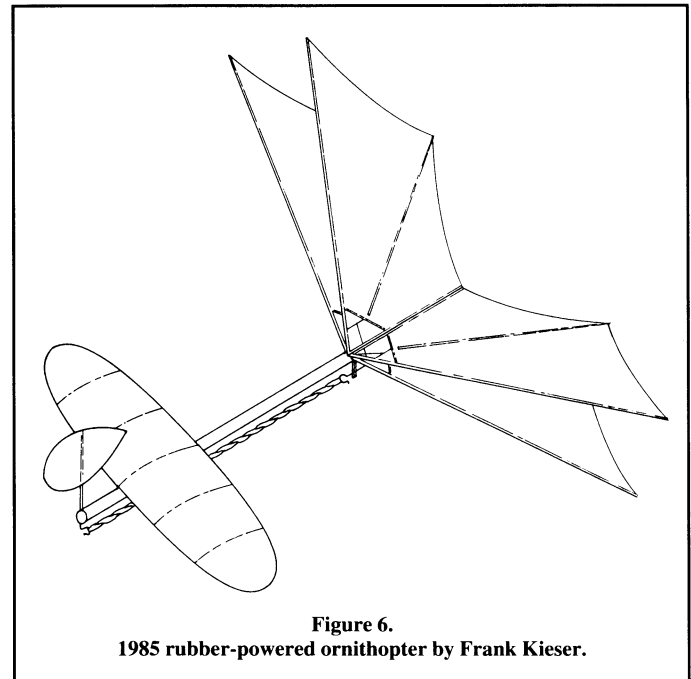
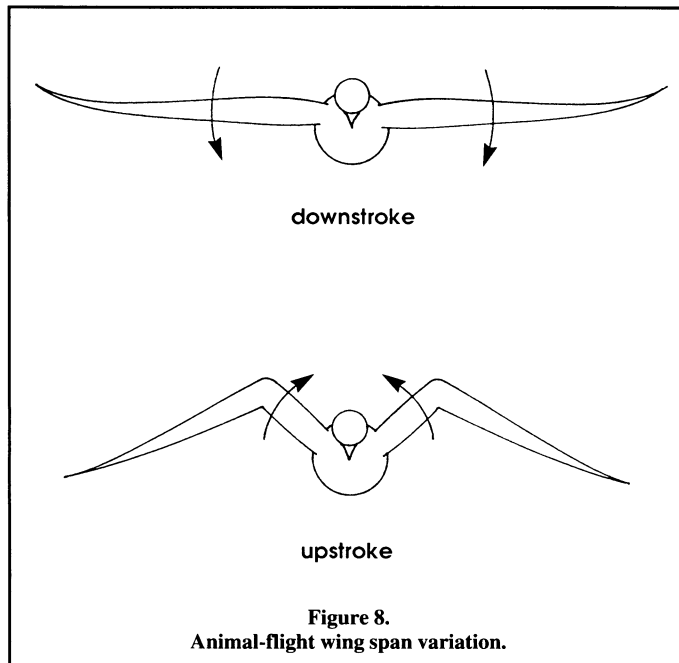
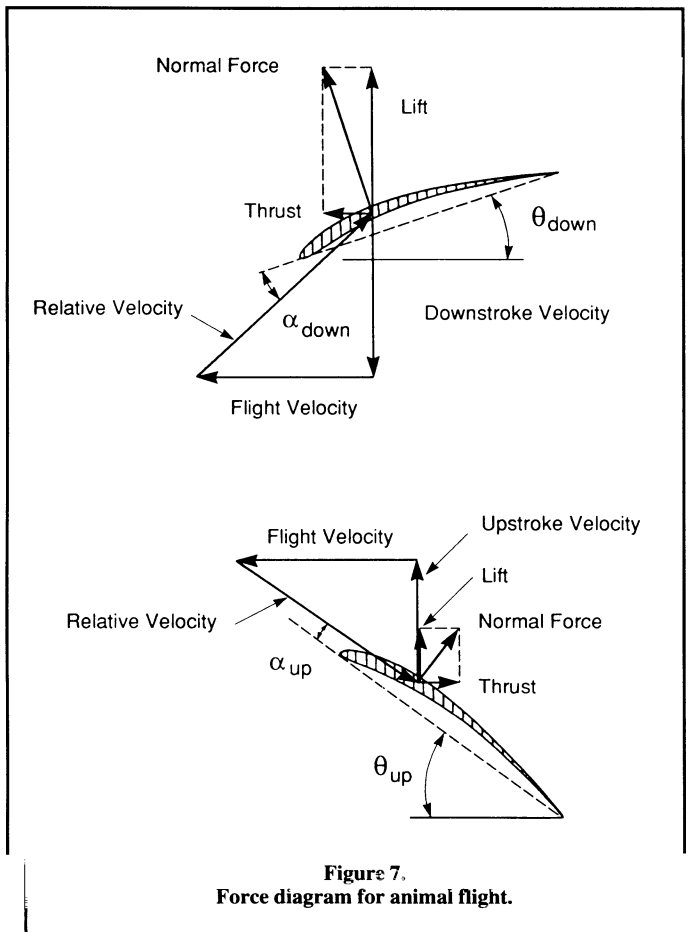


Figure 6.
1985 rubber-powered ornithopter by Frank Kieser.

aligned close to horizontal. This could produce an interesting dilemma for the upstroke. Namely, except for a certain average positive lift produced by a fixed camber, positive thrust on the upstroke will produce negative lift, and positive lift on the upstroke will produce negative thrust. Jeremy Rayner⁵ attempted to resolve this by postulating that birds and bats "collapse" their wings on the upstroke, thus producing neither lift nor thrust during that portion of the flapping cycle. However, subsequent research by Rayner and Geoffrey Spedding, as described and summarized by Lighthill,⁶ pointed out that the average lift will not equal the weight of certain example birds unless some lift is generated on the upstroke. The result of this thinking is an explanation of a kinematic phenomenon often noted in bird and bat flight, namely, the wings are partially folded during the upstroke to yield an effectively lower span than that during the downstroke (see Figure 8). Therefore, the upstroke produces negative thrust and positive lift (illustrated in Figure 7), but in smaller magnitudes than those during the downstroke. Net positive thrust is thus obtained.

Reference 6 further describes how the variable-span model allows flapping flight to be attained with constant bound vorticity.



ity throughout the flapping cycle. That is, no transverse, unsteady, vortex wake is shed with the attendant Theodorsen

- dD_c , a chordwise drag due to camber,
- dD_s , a chordwise drag due to skin friction, and
- dN_a , an apparent-mass force normal to the chord at the 1/2-chord location.

Adrian Hsieh⁸ the tasks of analytically studying the performance of a variable-span flapping wing. Stoll used a simple, planar, Prandtl lifting-line model, and Hsieh elaborated on this with an out-of-plane lifting-line model. In both cases, significant thrusts were produced for moderate span changes, with the two independent efforts giving comparable results.

Although neither Rayner nor Lighthill mention this, their variable-span model also answers a question regarding the efficiency of thin airfoils on a flapping wing. Reference 9 describes how thin, cambered airfoils provide a clearly optimum minimum-drag performance at a single value of lift coefficient. That is, such airfoils, with no leading-edge suction, are virtually single design-point sections. Thus, it never made a great deal of sense that nature would require such sections to experience a large range of lift coefficients throughout the flapping cycle. Furthermore, wind-tunnel tests¹⁰ showed that these airfoils have a limited angle-of-attack range for attached flow.

With the constant bound-vorticity model, however, these airfoils can operate within a narrow range of lift coefficients about the optimum (the lift coefficient varies even if the vorticity is constant because the local relative velocity varies throughout the flapping cycle). Also, from Reference 7, the calculated magnitudes and phases of the spanwise pitching distributions are comparable to those observed from bird-flight measurements. Because such motions are largely driven by aeroelastic reactions to the flapping, it may be possible to mechanically replicate this, in a straightforward fashion, for an ornithopter wing. In fact, this is probably the only way to obtain efficient bird-like flapping flight for small models where the airfoils, suitable for their speed regime, will typically offer low leading-edge suction efficiency.

For larger-scale ornithopters, however, where higher Reynolds number flow allows the incorporation of double-surface airfoils with high leading-edge suction efficiency, one may design an efficient wing that retains the traditional mechanical simplicity of constant-semispan flapping. Such a wing was developed for the successful engine-powered ornithopter shown in Figure 9, and the balance of this paper will describe its features.

DESIGN FEATURES

Aerodynamic Model

The wing's aerodynamics are modelled by a modified strip-theory approach where the forces on each section (shown in Figure 10) are determined solely by the local parameters, except that the steady-state downwash and unsteady shed wake effect are approximately accounted for through the wing's finite aspect ratio. A detailed analytical description is given in Reference 11, but this will be summarized in this paper as follows. First, the section operates in one of two distinct flight regimes: stalled or unstalled. This is determined by the relative angle of attack at the leading edge, with a dynamic-stall delay effect accounted for. For the unstalled state, the parameters determining the forces include the section's geometry, relative angle-of-attack at the 3/4-chord location, pitching rates, and dynamic pressure at the 1/4-chord location. The resulting forces, shown in Figure 10, are:

- dN_c , a force normal to the chord at the 1/4-chord location;
- dT_c , a chordwise leading-edge suction force;

function by reflection on the lift and thrust. This is a hypothesis, quite at variance with the constant span flapping assumed by previous animal-flight research. In my fourth-year thesis topics, the author assigned Karl

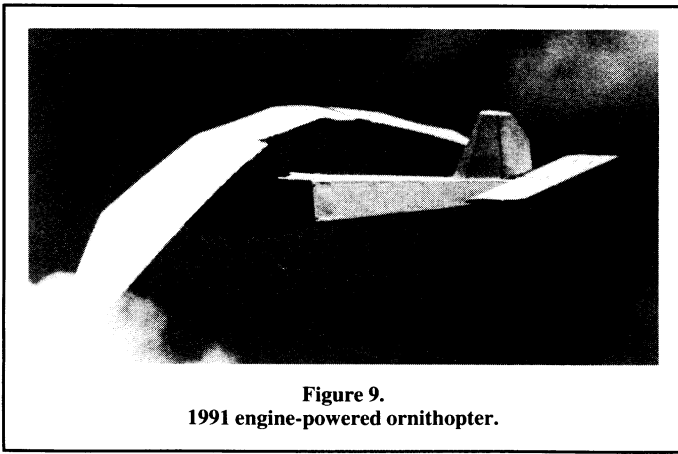


Figure 9.
1991 engine-powered ornithopter.

For the stalled regime, the key motion parameters are the midchord normal velocity and its time derivative, which produce the separated-flow forces:

- $(dN_c)_{sep}$, the midchord cross-chord force; and
- $(dN_a)_{sep}$, an apparent-mass force that is assumed to be $1/2 dN_a$.

It is seen how the normal force could act in a fashion similar to that previously discussed for the Pénaud ornithopter and animal flight, in that its forward tilt would give thrust. However, thrusting may also be obtained from the leading-edge suction when the flow is non-stalled. It was found, in fact, that efficient constant-semispan flapping is best obtained by cyclically twisting the wing only just enough to prevent stalling, so as to allow the leading-edge suction to reach its largest possible value. A cycle history¹² for a wing's outboard segment where the leading-edge suction efficiency was 91% is shown in **Figure 11**.

Even with the drag forces accounted for, the resultant vector has a forward tilt relative to the chord throughout most of the cycle, thus producing positive thrust during the downstroke and upstroke. Negative lift is produced during the upstroke, but the larger positive lift during the downstroke results in a net positive lift. By comparison, with zero leading-edge suction, the net lift would have remained approximately the same, but the net thrust would have been negative.

Finally, the sectional forces may be integrated along the wing's span to obtain the total instantaneous values of thrust and lift throughout the flapping cycle; and these, in turn, may be integrated throughout the cycle to obtain the average thrust and lift. Further, Reference 11 also shows how these forces, along with calculated pitching moments, may be used to obtain the instantaneous and average input and output powers. From this information one may readily calculate the wing's propulsive efficiency,

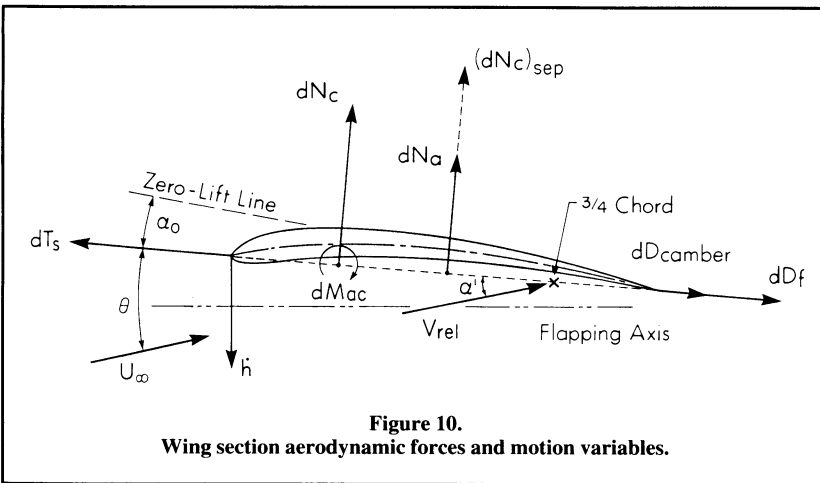


Figure 10.
Wing section aerodynamic forces and motion variables.

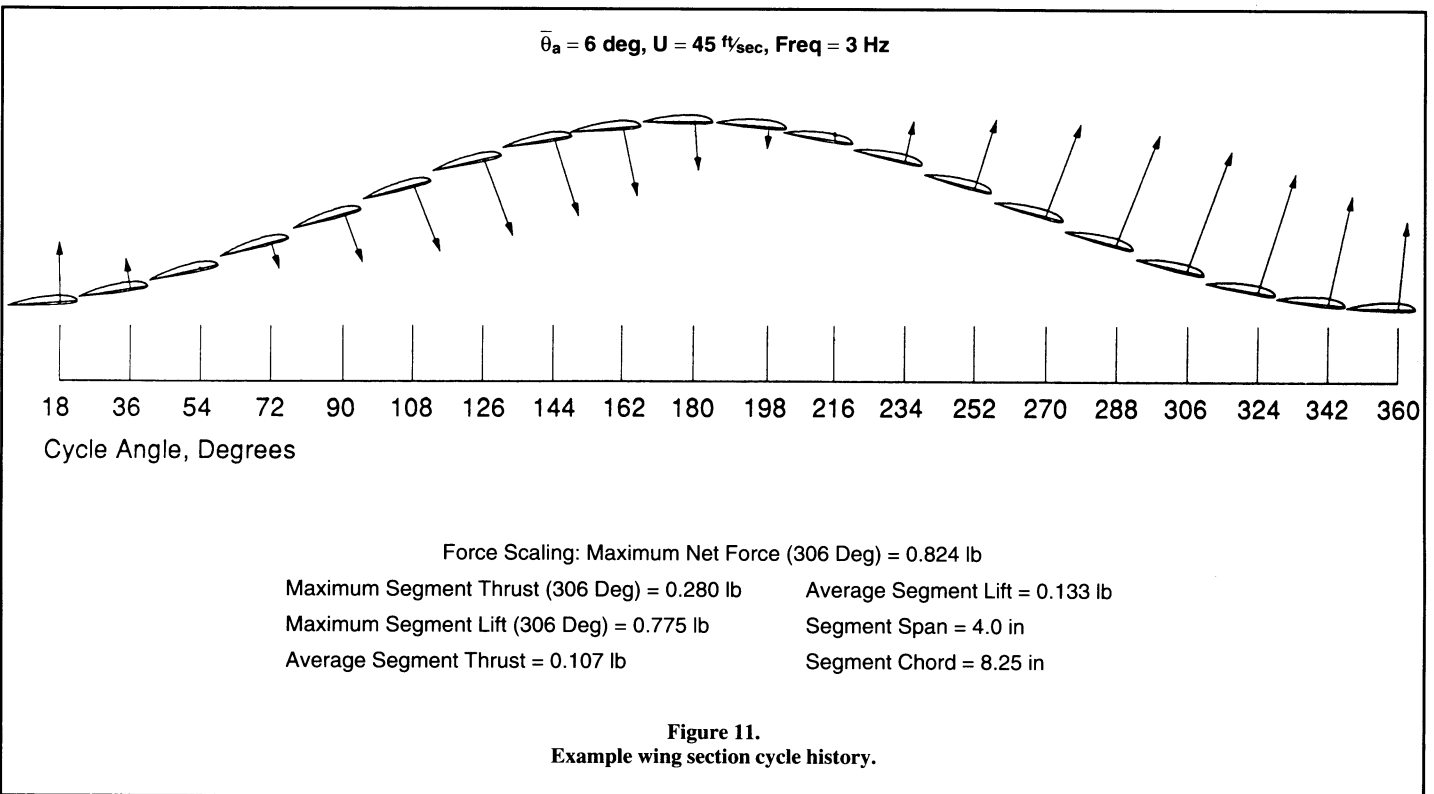
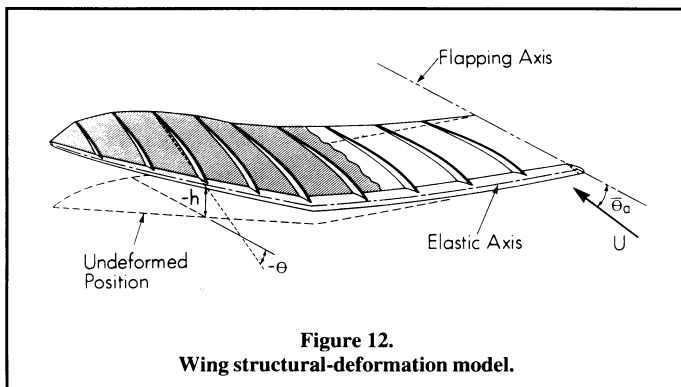


Figure 11.
Example wing section cycle history.

which is a measure of the flight efficiency of this type of constant-semispan flapping wing.

Aeroelastic Tailoring

In **Figure 10**, one sees that the motion of each section along the span consists of a plunging velocity, h , and pitching, θ . The manner in which this motion is imposed outboard of the flapping axis is represented in **Figure 12**, where flapping about this fixed axis, along with the corresponding aeroelastic distributions of bending and twisting, determines the motions at each spanwise station. That is, the only aspect of the flapping action that is directly driven by the mechanism is the cyclic dihedral angle at the axis. If the wing were perfectly rigid, it would then flap up and down at the same angle as at the axis, like a hinged plank. However, the designed flexibility of the wing means that it will bend and twist in response to the aerodynamic and inertial reactions of the flapping.



As previously discussed, a certain amount of pitching motion is required for efficient performance. Since this isn't directly driven, the wing must be designed to produce that pitching through its aeroelastic twisting response. The type of structure capable of achieving this (shown in **Figure 12**) is similar to the Pénaud wing in that the main structural element is a single spar along the leading edge. Firmly attached to this are rigid ribs, so that the spar may be elastically twisted by loads from the wing's surface transmitted through the ribs. The surface covering has such bending compliance that the wing's overall elastic axis is the same as that of the spar alone. The aerodynamic and mass centres are thus aft of the elastic axis, and hence capable of producing twisting moments.

A discrete-element analysis was developed, called "ComboWing," which modelled the elastic properties through a matrix of structural flexibility influence coefficients. The aerodynamic loading was based on the attached-flow sectional model previously described; and inertial-reaction loads were also included. As discussed in Reference 12, ComboWing calculated the magnitudes and phases of the bending and twisting motion in response to the imposed flapping, and allowed the effects of various design parameters to be assessed.

It was found that the wing gave its best performance when the pitching lagged the flapping by approximately 90° . The aerodynamic loads, alone, act to give this phasing. However, the inertial-reaction loads tend to drive the phasing away from this, towards 180° , which severely degraded the performance. Therefore, an important result from the analysis was that the mass aft of the elastic axis should be kept as light as possible.

The magnitude of the twisting had to be kept within a certain range in order to give good performance. For example, too little twisting would cause massive stalling and too much twisting could cause the wing to act in a "windmilling" mode, actually taking energy from the flow. The primary design features used to control the twisting magnitudes were: the spanwise distribution of the spar's torsional stiffness, GJ ; and the sweepback of the wing's outer portion, which provides additional torque and corresponding twist on the inner portion (a feature also seen on animal wings). Thus, the design process for obtaining the optimum performance for this type of ornithopter wing could best be described as a version of "aeroelastic tailoring."

A consequence of the wing's torsional compliance was that the average flight loads could give an excessive, and inefficient, mean washout if the wing were built "flat." This washout, along with its corresponding mean bending, is the "static" deformation, upon which the dynamic motions are superimposed. It was therefore necessary to build in a certain amount of pre-twist in order to obtain best performance.

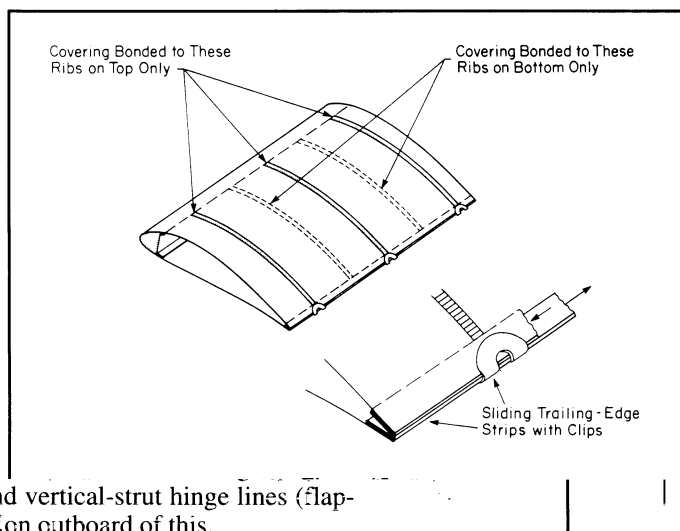
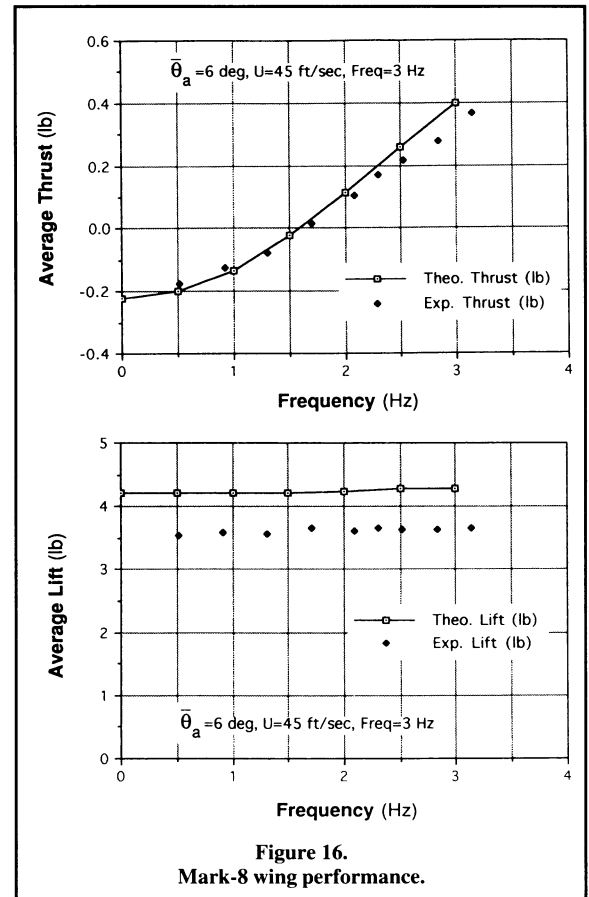
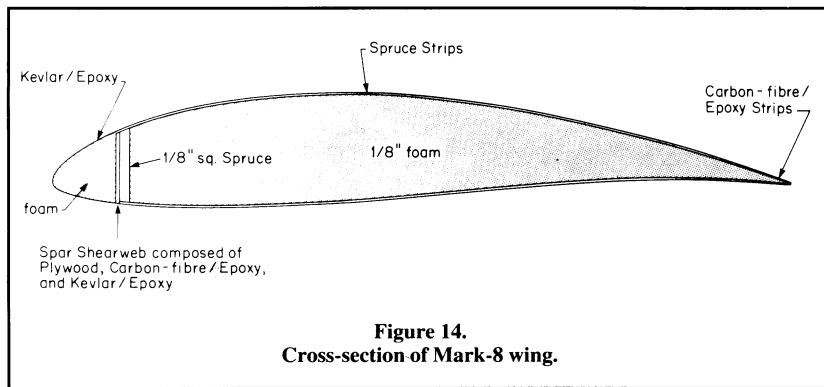
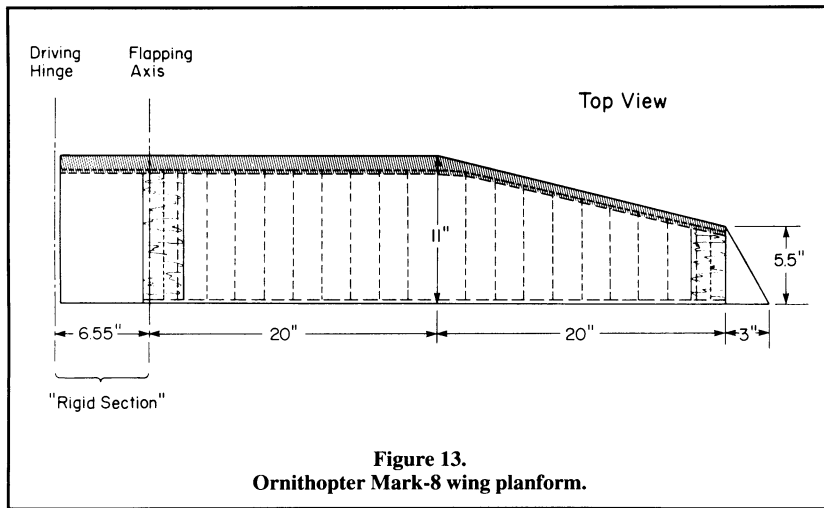
Finally, it was found that the bending dynamic response should be suppressed for efficient performance. That is, excessive dynamic bending (whipping) would cause considerable reduction in thrusting. However, when the spar's bending-stiffness distribution, EI , was above a certain reasonable threshold value, the adverse effects from this became negligible. Therefore, the design requirements for the spar included a fair amount of bending stiffness along with torsional compliance. Further, this had to be accomplished with a structure that was light and strong. The next section describes how this was achieved with composite construction.

Construction

Figures 13 and 14 show the layout and cross-section of the "Mark-8" wing panel, which was the culmination of a long design evolution described in Reference 12. The composite spar design incorporates a plywood and carbon-fiber shear web to provide bending stiffness and strength; and the torsional characteristics are largely determined by the cross-sectional shape formed by a Kevlar/epoxy surface surrounding a foam core. The warp fibers of the Kevlar cloth are parallel to the span to allow torsional compliance to be achieved by a spar with a sufficiently deep shear web.

A special feature of this wing's structure is that it is able to provide the required torsional compliance while, at the same time, incorporating efficient double-surface airfoils designed by Prof. Michael Selig of the University of Illinois. **Figure 15** shows how this is accomplished, where the closed "torsion box" normally formed by the thick airfoil is opened by splitting the trailing edge. That is, this feature (patented as the "Shearflex Principle") allows a double-surface wing to have the high torsional compliance of two single-surface wings joined at the leading edge. For example, the Mark-8 wing easily twists even though its lightweight covering does not readily stretch. In fact, shearflexing would work well even if the skin was thick and relatively inflexible. Therefore, a rubber-like covering is not needed for the structure to have torsional compliance.

The structural-continuity requirements of shearflexing compel the twist distribution to vary linearly with span. Hence, the composite spar cross-section, shown in **Figure 14**, must be carefully sized along the span to give the requisite GJ distribution. It was also found that in order to achieve twisting linearity all the way out to the tip, without the spar size, and strength, going to zero at that point, extra aerodynamic help was required from a rigid triangular tip portion.



very favourable; and, most importantly, they showed that the ornithopter was capable of sustained flight with these wings. In fact, this was a fairly conservative conclusion given that the tests were conducted with the flapping-axis angle at 6° , which was the value necessary for the shearflexing portion, alone, to produce sustaining lift for the entire ornithopter.

Incorporation into the Ornithopter

The ornithopter's configuration, where one sees that the complete wing consists of three components ("panels"), is shown in **Figure 17**. The centre panel is designed to be rigid, and is driven in a sinusoidal non-pitching fashion from the fuselage (for details of the drive mechanism see Reference 13). The two outer panels are hinged to the centre panel so that they may be rocked upon the two, hinged, vertical struts. As previously described, the outer panels themselves consist of a rigid portion

Figure 15.

Structural design for shearflexing.

anges and vertical-strut hinge lines (flap-
portable portion outboard of this.

ing design was invented by the author's
y Harris. The intention was that, because
were moving in opposite directions, this
portunity to balance the net inertial and
mitted to the fuselage. In practice, this
tained; however, this wing does achieve
of the net unbalanced force compared
onal root-flapping wing. This is an impor-
full-scale ornithopter where a pilot would
al shaking accelerations be kept within

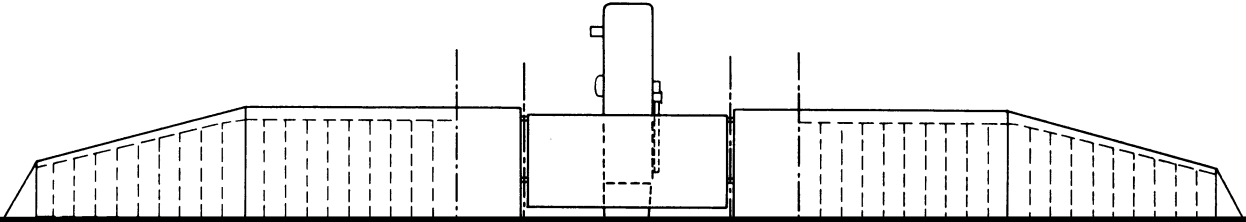
Because of the overall wing-drive kinematics, described in the next section, the wing panel required a "rigid section" between the driving hinge and flapping axis. The shearflexing portion was accommodated by allowing its upper surface to freely slide over the upper surface of the rigid section.

Wind-tunnel experiments were conducted on one wing panel.¹² The comparisons between test results and ComboWing predictions for average thrust and lift are shown in **Figure 16**. Considering the approximations in the ComboWing analysis and limitations of the experimental technique, the comparisons are

between the driving hi
ping axes), and a flexib

The three-panel w
project partner, Jeremy
portions of the wing v
would afford an oppo
aerodynamic loads tran
is far from perfectly at
a significant reduction
with that for the traditio
tant consideration for a
require that the vertica
tolerable limits.

Support struts not shown



Another feature of the three-panel wing is that it acts to even out the instantaneous power needed to flap it. That is, ornithopter engines are sized in accordance with the peak power required. For a traditional root-flapping wing, the power required for the downstroke can be considerably higher than that for the upstroke, thus necessitating a much larger engine than that which would have been chosen from average-power considerations alone (as is the case for a propeller-driven airplane). One way in which the peak power may be reduced is to store some of the upstroke energy, and then release it to assist the downstroke. This was accomplished, for example, by AeroVironment Inc. in their robot flying pterosaur project,¹⁴ by storing energy in bungee cords hidden within the “creature’s” neck.

In an ideal three-panel wing, the maximum values of upstroke and downstroke power could be made equal, thus minimizing the requirement for any energy-storage device. The amount that the engine has to be oversized depends on the degree to which the wing varies from this optimum case. In fact, the maximum engine power for the 3 m-span ornithopter was twice that of the calculated peak value required. This might well have been more than needed: the aircraft did fly with no energy-storage except that provided by the rotational inertias of the engine and drive mechanism. However, for a full-scale ornithopter, it would be worth considering the combination of a certain amount of energy storage along with the three-panel wing.

Finally, it should also be noted that recent model ornithopter designs have been using multiple wings, oscillating out of phase, to smooth out the torque requirements from the driving rubber-band motor. This distinctly non bird-like approach has the additional benefit of balancing the oscillating lift. As described by Phillips,¹⁵ excessive fuselage heave can seriously degrade the aerodynamic performance for such lightweight aircraft. This may well be a factor in the recent dramatic increase in duration times for model ornithopters, now over a quarter of an hour for flight in a large enclosed space.

PERFORMANCE

The design and predicted flight performance of the 3 m-span ornithopter was based on ComboWing analyses, in conjunction with the wind-tunnel experiments on the single wing panel. The resulting flight tests were very successful, with the aircraft easily sustaining and climbing until it was decided to land (further details of these, and previous flights, are described in Reference 13). However, it was observed that the aircraft flew with its flapping axis aligned horizontally, whereas ComboWing predicted a required angle of 6°. Clearly, ignoring the contributions of the rigid portions and centre panel was far more conservative than needed. It was therefore decided, after the fact, to extend the ComboWing analysis to predict the flight performance of the complete three-panel wing.

The program, called “FullWing,” yielded some interesting and useful results. First, it confirmed that the lift contributions of the rigid portions and centre panel were, as the flight tests had indicated, sufficient to allow sustained cruise with the flapping axis horizontal. Second, it showed that although their net or surplus thrust was close to zero, the oscillating rigid portions and centre panel produce enough gross thrusting effort to effect a substantial reduction in their own drag. In addition, they indirectly contribute to the overall performance of the whole wing because the lower flapping-axis angle allows the outer panels to operate more efficiently and maintain better stall margins.

From FullWing, nominal equilibrium flight was predicted at a flapping-axis angle of -0.5°, a flight speed of 45 ft/s, and flapping frequency of 3 Hz, with the wing performing as summarized below:

- Average Lift = 8.61 lb
- Average Thrust = 0.88 lb
- Maximum Unbalanced Lift = 6.35 lb
- Average Propulsive Efficiency = 54%

By comparison, it was estimated from a frame-by-frame study of the flight videos that a typical speed was approximately 50 ft/s at an average flapping frequency of ≈ 3.3 Hz. It was concluded that the aircraft was flown slightly “hot” by the pilot (who was probably exuberant at finally being provided with a flight-capable ornithopter).

Upon using the “what if” capabilities of FullWing, it was possible to compare the as-flown ornithopter with a hypothetical two-panel craft employing only the shearflexing portions. The results show that the three-panel configuration reduces the magnitude of the unbalanced lift by about two pounds. While this is a significant reduction, it is not close to complete cancellation because the design process for proportioning the panels always requires a resolution of aerodynamic and structural tradeoffs. However, if balance were the only consideration, it would be possible, in principle, to configure the panels for achieving a cancellation closer to 100%.

A dynamic-response analysis of the ornithopter has not been performed, so it is not known what value of fuselage heave should have resulted from the above-noted lift imbalance. However, from Reference 15, an ornithopter of this size and mass should have had very little perceptible vertical motion, which is exactly what was observed from the flight videos.

Finally, some important observations may be made regarding the propulsive efficiency. The 54% value may seem small in comparison to that for propellers, which is on the order of 80% when operating in this Reynolds number regime. However, the definition of ornithopter-wing propulsive efficiency, η , is:

$$\eta = \frac{\text{average thrust} \times \text{forward velocity}}{\text{average power required for flapping}}$$

where the average thrust incorporates the wing’s drag. In order for this efficiency definition to be comparable to that for a propeller, the non-flapping drag of the ornithopter’s wing must be subtracted from its average thrust. When this is done, the wing’s propulsive efficiency becomes 77%.

CONCLUDING REMARKS

As described in the introduction, there are various types of mechanical flapping wings, the classical example being the Pénaud membrane-surface design. The Pénaud wing’s efficiency can be improved by combining it with various fixed lifting surfaces, as well as by using multiple flapping surfaces. However, these all rely on the low advance-ratio thrust of the Pénaud flapper to produce lift, either by vectoring the thrust or propelling the fixed surfaces.

By comparison, the flapping wing described in this paper is designed to operate efficiently at higher advance ratios, producing sustaining lift while the thrust vector is horizontally aligned. That is, the average thrust propels the flapping wing to such a speed that lift is produced from its average aerodynamic geometry. This is analogous, in fact, to the way a horizontally-vectoring propeller acts to thrust a fixed wing to flight speed; the

overall propulsive efficiencies of the two types of flight are comparable.

This wing has several special features. First, it consists of three panels that move in such an opposing fashion that the net unbalanced oscillating lift felt by the fuselage is reduced. Also, the three-panel feature acts to even out the peak power required during the flapping cycle, reducing the need for any energy-storage devices. Second, the outer panels of the wing incorporate a structural feature by which they may have torsional compliance along with an efficient double-surface airfoil. In fact, it is the ability to use such an airfoil with its high leading-edge suction and attached-flow angle-of-attack range that is the key to the wing's performance. However, this is only achieved if the dynamic twisting in response to the flapping is close to certain values of magnitude and phase. This is controlled by aeroelastic tailoring, where the spar is designed to have a torsional-stiffness distribution prescribed by an analysis that predicts the wing's structural-dynamic response.

Finally, this wing was incorporated into a proof-of-concept remotely-piloted ornithopter that demonstrated successful sustained flight. The performance, as deduced from the flight videos, matched the predicted flight characteristics. That is, the aircraft flew within a range of flight speeds and flapping frequencies close to those values obtained from the analysis. Further, it was clear that there was more than sufficient power, so that the ornithopter was flying with generous margins. It has been shown that this wing design is capable of operating at a high propulsive efficiency, although, in practice, this is somewhat offset by the drag of the support struts and the weight of the drive mechanism. Nonetheless, as a qualitative observation, the aircraft's performance was comparable to that of a typical, well-designed, fixed-wing model of similar wing loading and power loading. These results, both experimental and analytical, provide encouragement that this particular solution to flapping-wing flight may be applicable to a successful full-scale ornithopter.

ACKNOWLEDGEMENTS

This research was partially supported by an Operating Grant from the Natural Sciences and Engineering Research Council of Canada. Jeremy M. Harris, Principal Research Engineer at Battelle Memorial Institute and the author's partner in the ornithopter project, carefully monitored the technical content of the article as it was being written, as well as producing **Figures 11** and **15**. Also, this article benefitted greatly from proofreading by Chris Hayball (of de Havilland Aircraft) and Nessa Olshansky-Ashtar, who made this much more readable and accurate.

REFERENCES

- ¹Lippisch, Alexander M., "Man Powered Flight in 1929," *Journal of the Royal Aeronautical Society*, Vol. 64, July 1960, pp. 395-398.
- ²Gibbs-Smith, C.H., "The Eighteen Seventies and Eighties," *A History of Flying*, B.T. Batsford, London, 1953, page 172.
- ³Stephenson, Jack, Private Communication, 1993.
- ⁴Archer, R.D., Sapuppo, J., and Betteridge, D.S., "Propulsion Characteristics of Flapping Wings," *Aeronautical Journal*, Vol. 83, September 1979, pp. 355-371.

⁵Rayner, J., "A Vortex Theory of Animal Flight. Part 2. The Forward Flight of Birds," *Journal of Fluid Mechanics*, Vol. 91, Part 4, 1979, pp. 731-763.

⁶Lighthill, Sir James, "Some Challenging New Applications for Basic Mathematical Methods in the Mechanics of Fluids that were Originally Pursued with Aeronautical Aims," *Aeronautical Journal*, Vol. 94, No. 932, February 1990, pp. 41-52.

⁷Stoll, Karl, *Analysis of the Lighthill Model of Animal Flight*, Division of Engineering Science, Faculty of Applied Science and Engineering, University of Toronto, Thesis for the Degree of Bachelor of Applied Science, 1991.

⁸Hsieh, T.C., *Analysis of the Constant-Circulation Model of Animal Flight Using Discrete Lifting-Line Method*, Division of Engineering Science, Faculty of Applied Science and Engineering, University of Toronto, Thesis for the Degree of Bachelor of Applied Science, 1992.

⁹DeLaurier, J., "Drag of Wings with Cambered Airfoils with Partial Leading-Edge Suction," *Journal of Aircraft*, Vol. 20, No. 10, 1983, pp. 882-886.

¹⁰DeLaurier, James D., "An Experimental Study of Low Reynolds Number Aerodynamics; Proceedings of the Conference on Low Reynolds Number Aerodynamics," Springer-Verlag, Berlin, 1989, pp. 173.

¹¹DeLaurier, J.D., "An Aerodynamic Model for Flapping Wing Flight," *Aeronautical Journal*, Vol. 97, No. 964, April 1993, pp. 125-130.

¹²DeLaurier, J.D., "The Development of an Efficient Ornithopter Wing," *Aeronautical Journal*, Vol. 97, No. 965, May 1993, pp. 153-162.

¹³DeLaurier, J.D. and Harris, J.M., "A Study of Mechanical Flapping-Wing Flight," *Aeronautical Journal*, Vol. 97, No. 966, October 1993, pp. 277-286.

¹⁴Brooks, A.N., MacCready, P.B., Lissaman, P.B.S., and Goman, W.R., *Development of a Wing-Flapping Flying Robot for the Largest Pterosaur*, AIAA Paper 85-1446, 1985.

¹⁵Phillips, Hewitt, "The Fuselage Motion of Ornithopters," *Eighteenth Annual Symposium Report of the National Aeronautics and Space Administration*, 1985, pp. 49-53.